Investigation of Local Electrochemical Performance and Local Degradation in an Operating Solid Oxide Fuel Cell

Zacharie Wuillemin[1], Andres Müller[1], Arata Nakajo[1], Nordahl Autissier[1], Stefan Diethelm[1], Michele Molinelli[2], Jan Van herle[1], Daniel Favrat[1]
[1]Ecole Polytechnique Fédérale de Lausanne
Laboratoire d'Energétique Industrielle (LENI)
Station 9
CH-1015 Lausanne
Tel: +41-21-693 35 49
zacharie.wuillemin@epfl.ch

[2]HTceramix – SOFCpower
CH-1400 Yverdon-les-Bains

Abstract

In order to characterize a new SOFC stack design, to investigate degradation processes and to validate models, a diagnostic test station was designed and realized. It allows to characterize repeat-elements locally by measuring the local potential, current density and temperature over the active area. The active area is segmented in 18 small electrically insulated measurement points (segments), in addition to a main segment.
The profile of current density was investigated up to an average of 0.6A/cm2 and 67% of fuel utilization, showing as expected a different response depending on the position along the flowpath. In addition, the local Nernst potentials were measured by temporarily disabling the polarization of the concerned segments. The temperature profile was also investigated as a function of the output current, showing a large heat transfer with the test furnace in this single-element configuration.
In addition, local degradation behavior was studied over 1900 hours. In particular, it was found that the repeat-element showed a large sensitivity to fuel composition, with larger degradation rates under pure hydrogen than under diluted fuel mixture. Impedance spectroscopy results showed large differences in degradation behavior, depending on the location in the repeat-element and on the polarization history. In particular, segments that had not been polarized during the test showed lower ohmic resistances than the polarized ones, and zones located near the gas inlets degraded more than those near the outlet.
With this experiment, it was clearly demonstrated that degradation processes depend on local operating conditions.

Introduction

The understanding of degradation processes is of key importance for the development of solid oxide fuel cells. These processes are often investigated at the scale of separate components (electrodes, electrolyte, cell, MICs, seal materials) or in repeat-element and stack configuration. The first approach allows to separate contributions from various sources, and the second represents a coupling of the various degradation sources at the stack level, in addition to those coming from system components.
The difficulty to understand and predict the overall degradation of a fuel cell repeat-element and stack partly lies in the fact that the local gas composition, the local

temperature, the local current density vary along the flow path in a repeat-element, all parameters having an influence on degradation.
It is therefore probable that the local operating conditions in a fuel cell repeat-element imply different local degradation mechanisms and degradation rates. Moreover, some degradation sources such as pollutant species are transported by convection and diffusion, and therefore locally depend on upstream conditions and components.
In order to investigate these interactions, but also with the goal to investigate the performance of a new fuel cell prototype and to validate models, a diagnostic test station was built which allows to perform a local characterization of the electrochemical performance and of the operating conditions in a fuel cell.
After a description of the diagnostic setup, investigations on the local electrochemical performance are presented. The evolution of the test over 1900hrs is detailed, showing local degradation behavior. Finally, impedance spectroscopy results are used to give more details in the differences in local degradation.

Experimental setup

In the framework of the FP7 European Project FLAMEsofc, a new 2.5kWel-class stack was designed at EPFL's *Industrial Energy Systems Laboratory* (LENI), in collaboration with HTceramix - SOFCpower. The new stack consists of planar anode-supported cells with an active area of 200cm^2, supplied in air and fuel by external manifolds in a co-flow configuration (Figure 2). The gas diffusion layers (GDL) are made of SOFConnex^{TM} provided by HTceramix.

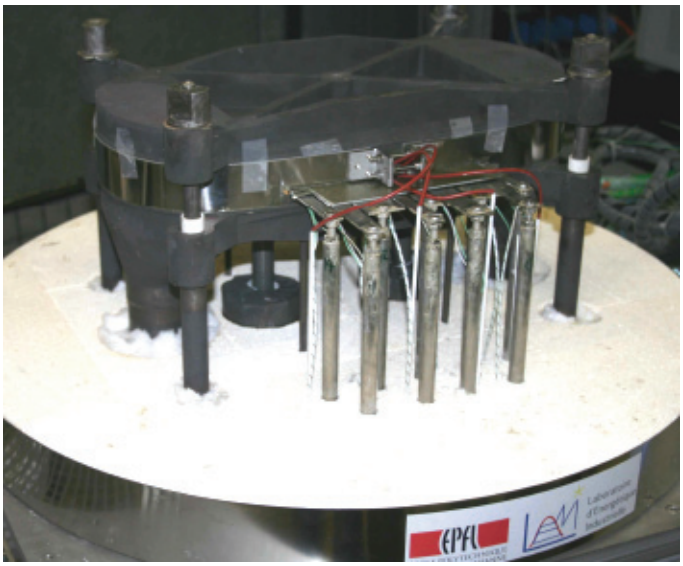

Figure 1: diagnostic setup for the FlameSOFC design

Due to its large active area, this stack design is well suited for local investigations. However, the diagnostic test station is capable to receive other fuel cell stack designs. In the present case, the experiment is made in the same configuration as for a real stack or repeat-element test, but with additional instrumentation.

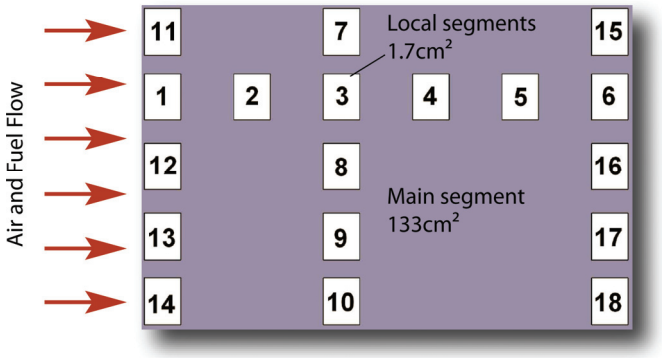

Figure 2 Disposition of the segments on the active area

The local characterization is performed by separating the active area of the cell in electrically independent areas called segments (Figure 2), in a similar manner as presented by Ravussin et al. [1] and Metzger et al. [2]. The active area of the cell is segmented by screen-printing separate cathode areas. In the presented experiment, a total number of 18 segments of 1.7 cm^2 active area each were distributed on the surface, in addition to a large main segment of 133 cm^2. The segments were organized as one 6-segment line along the flowpath, and three 5-segment columns perpendicular to the flow path (see Figure 2). The inlet and outlet segments are used to verify the gas composition, fuel distribution and mass balance. The horizontal line is used to get a precise profile of temperature and current density along the flow path.

The cathode MIC consists of a main plate connected to the main active area of the cell, and additional electrically insulated parts for the segments. The segments are composed of a contact area, a current collection bar, a potential wire and a thermocouple inserted in the gas channel of the gas diffusion layer (GDL) (see Figure 3).

In the present test, the metallic interconnects (MIC) were made of UGINE F18TNb alloy. Due to the production process and time constraints, it was not possible in this experiment to coat the alloy with a protective coating on the cathode side to avoid chromium evaporation.

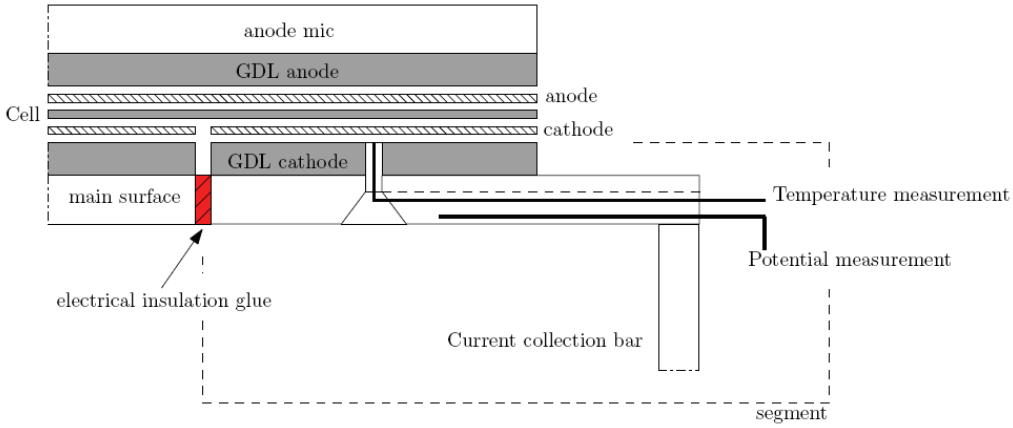

Figure 3: Segmentation of the cathode MIC with instrumentation

The diagnostic repeat-element was mounted in a dedicated test setup (Figure 1). The current collection bars, the 19 potential wires and 19 thermocouples were passed through the insulation of the oven and connected to the instrumentation.

The instrumentation is connected to a computer that controls the test station. The repeat-element can be fed with humidified hydrogen, syngas and methane for steam-reforming or partial-oxidation.

The main segment is connected to a power supply and to a 150A computer-controlled active-load. The 18 segments are connected to two multi-channel active loads, in order to

set a constant cell potential over the total area. The second multi-channel active load allows to temporarily disable the polarization on separate segments, in order to measure the local open circuit voltage (OCV) as a measurement of local Nernst potential and indirectly of the local gas composition. This is used to verify the integrity of the seals, to investigate the quality of the fuel distribution over the active area, and to measure the local cell overpotential. The diagnostics are completed by an electrochemical impedance spectroscopy (EIS) device (Zahner, IM6), which can be connected to individual segments.

For the present experiment, an anode-supported cell provided by HTceramix-SOFCpower was used, on which a LSM-YSZ cathode and a LSC current-collection layer were screen-printed. The experiment was assembled, verified and heated up at 2K/min up to 800°C. After verification of the gas tightness under pure nitrogen using a volumetric flowmeter the cell was reduced in a H2-N2 mixture for 3 hours. The rise in potential occurred successively on the various segments, following the flow direction.

Test overview

OCV

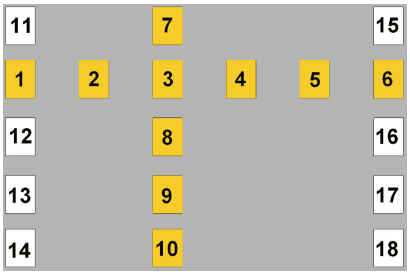

Figure 4 Identification of the polarized segments (yellow)

For a 6 SMLPM/cm^2 fuel mixture of humidified hydrogen (3% H_2O), the OCV of the main segment was 1075mV. The local OCVs decreased along the fuel flow path, from 1079mV at the inlet to 1069mV at the outlet. This decay could be explained by pinholes in the electrolyte, or by a residual leakage current through the electrolyte, resulting from a residual electronic conductivity [3]. The local OCV along the seals (segments 7,10,11,14,15,18, in Figure 4) showed values in the same range, indicating a correct behavior of the seal system.

Polarization

The repeat-element was polarized in a series of iV-characterizations and then operated at constant current for 1900 hrs with some interruptions for additional iV-characterizations and impedance spectroscopy measurements. Due to a failure of one multi-channel active load, eight segments (n°11-18) could not be polarized and remained at open circuit during the whole test, except when tested by EIS. It will be shown later that this failure allowed to investigate the effect of polarization on degradation, giving precious additional information. The polarized segments are shown in Figure 4. The segments n°1 to 10 were controlled in potentiostatic mode following the main segment (see Figure 5), while measuring the resulting local current density.

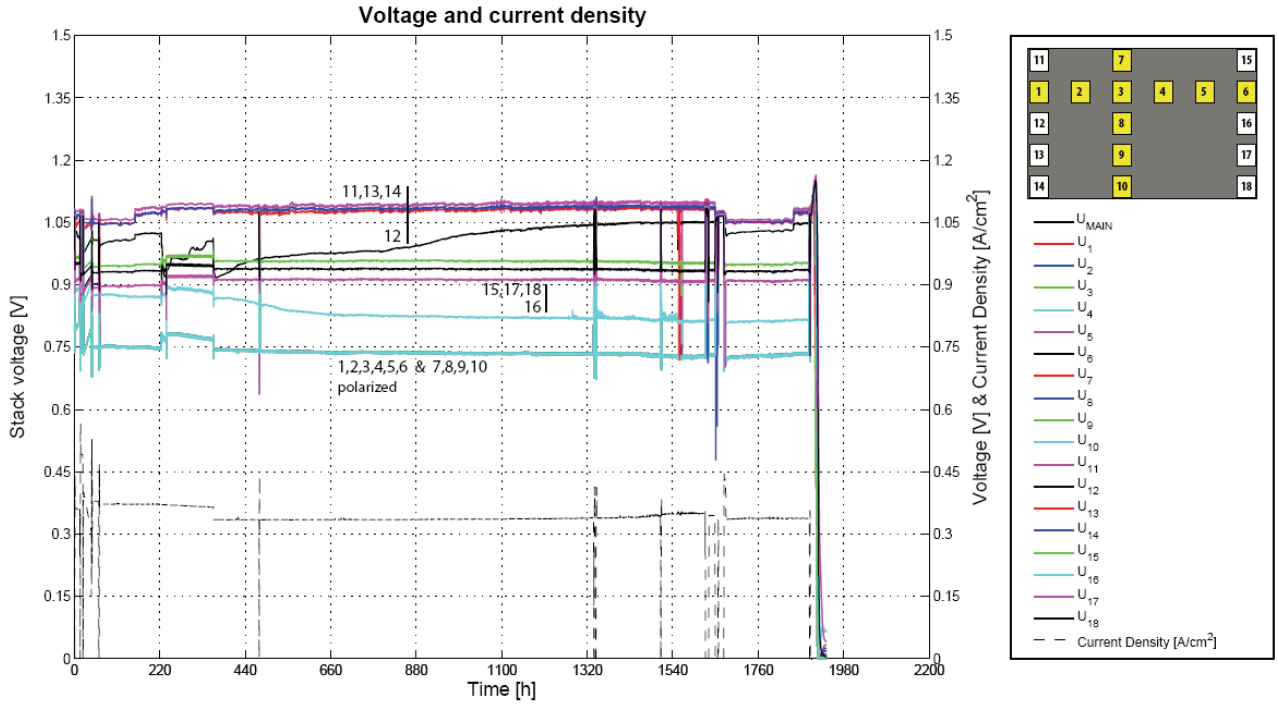

Figure 5: Overview of the 1900 hours of diagnostic test

It is known that degradation phenomena strongly depend on test history, in terms of successive operating conditions. In order to be able to make a link between local operating conditions, local recorded degradation and local post-experiment analysis (microstructure, chemical composition, pollutants, delaminations, cracks...), it was decided to keep the local conditions as constant as possible over the whole test. The drawback is the lack of data for the sensitivity of degradation to the operating conditions during the test, but the expected advantage should be a higher contrast in the local post-experiment analysis due to constant conditions and avoidance of overlapping 'history effects'.

The test was therefore mostly operated at constant fuel mixture of 6 SMLPM/cm2 hydrogen + 6 SMLPM/cm2 nitrogen (+ 3%H_2O) , with an average current density varying between 0.37 and 0.45A/cm^2. During a period of 130 hours, the nitrogen supply was stopped, showing an increased performance under 97% H_2, but a much higher degradation rate, as shown thereafter (Figure 9).

Air excess was λ=7 at the beginning of the test, a little less than the lambda of 8 required in the FlameSOFC project to keep the stack within a 100K operating temperature range at nominal power output. The oven temperature was kept at 800°C for the whole duration of the test.

Figure 5 shows the evolution of the potential of the segments over time. The potential difference between the polarized small segments and the main segment was within 4mV. At the inlet, the segments n° 11-14 remained at OCV. While segments 11,13 and 14 had close and stable potentials, segment 12 followed an erratic behavior with sudden drops of OCV after IV-characterizations and later increase over long periods. The causes for this behavior remain unclear, but it seems probable that it lies in a defect in the instrumentation. The same behavior was observed on the outlet (segments 15 to 18), where segment 16 showed a decrease in local OCV with time. In this particular case however, the drop of OCV could also indicate a degradation with time of the fuel flow distribution at the center of the element (lower flux), with an increasing apparent fuel utilization and a drop in Nernst potential.

Characterization

Local electrochemical performance

The evaluation of the local electrochemical performance was made by performing iV characterizations and measuring the local density on each segment, while keeping the cell potential constant on all segments.

Figure 6 shows the typical iV-characteristic of the segments disposed along the flow path, obtained after 63 hrs of operation under constant fuel and air fluxes. The best performance is obtained on segment 2. Segment 6, situated at the fuel outlet, shows a typical drop in current density below 0.75V cell potential, resulting from the local drop in Nernst potential due to increasing fuel utilization, and due to additional diffusion losses in the anode. The local output power density varies from 0.2 to 0.45 W/cm^2.

As shown thereafter by EIS (Figure 11), the unexpected low performance of segment 1 can be explained by a large polarization resistance, while the ohmic losses remain similar as for the other segments, hence excluding a contacting problem.

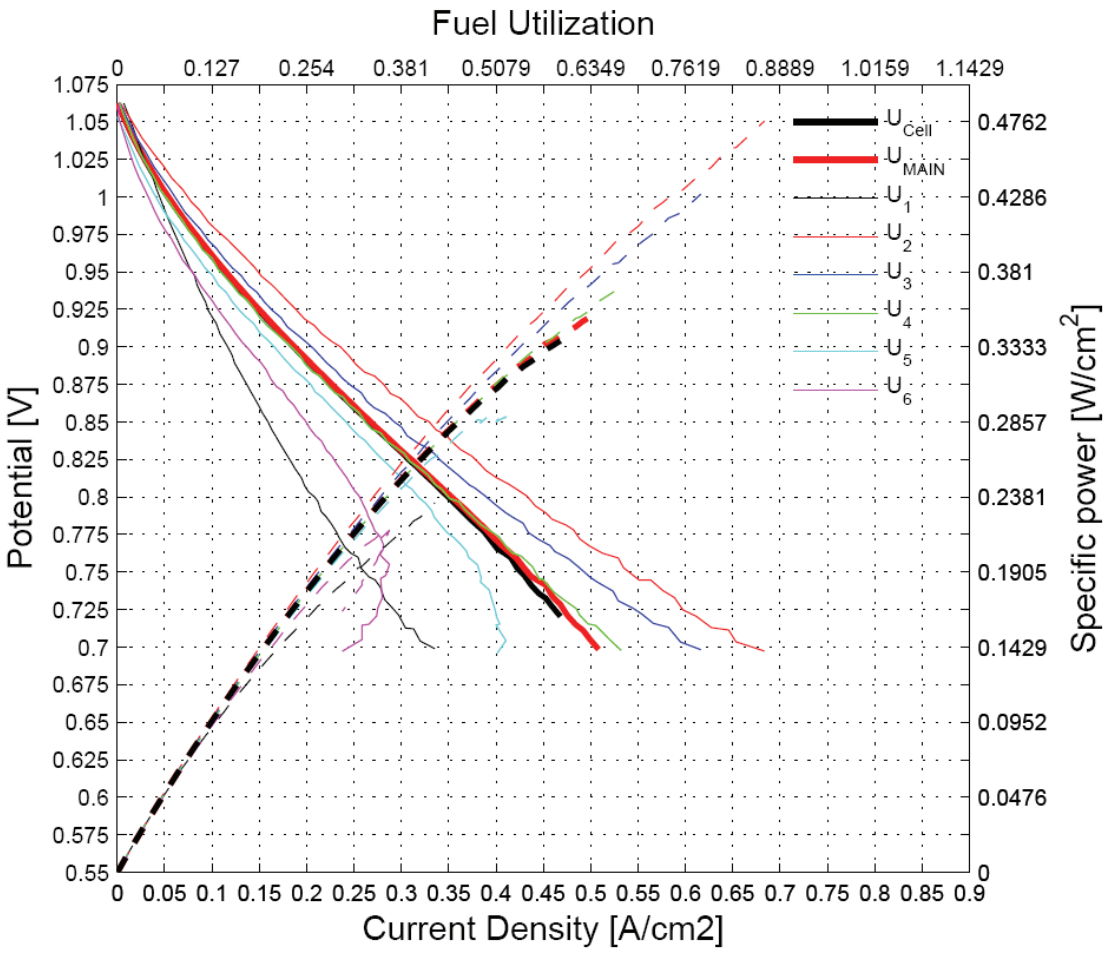

Figure 6 : i-V curve performed after 63 hours of operation . Fuel mixture: 6SMLPM H2 + 6 SMLPM N2 (+3% H2O). Segments of the horizontal axis.

Current density profiles

The current density profiles recorded at the beginning of the test (63 hrs) are shown in Figure 7, along with a comparison with modeling results for the same fuel utilization. The model, developed in house, is written for the FLUENT™ CFD software. Its description can be found in [4]. The electrochemical model was fitted by Nakajo et al. [5] on experimental data obtained in collaboration with Metzger et al. (Deutsches Zentrum für Luft- und Raumfahrt, Stuttgart, Germany) [2]. It allows to predict with accuracy the electrochemical performance of this type of cell, in a wide range of operating parameters, but before degradation.
Some discrepancies are therefore observed between model and experiment, especially on segment 1. Experimentally, the low current density on segment 1 induces a compensation on the other segments to maintain the same total current, explaining partly the differences between model and experiment. A bad contact on segment 1 could be excluded from impedance spectroscopy results (Figure 11), indicating another cause for low performance.

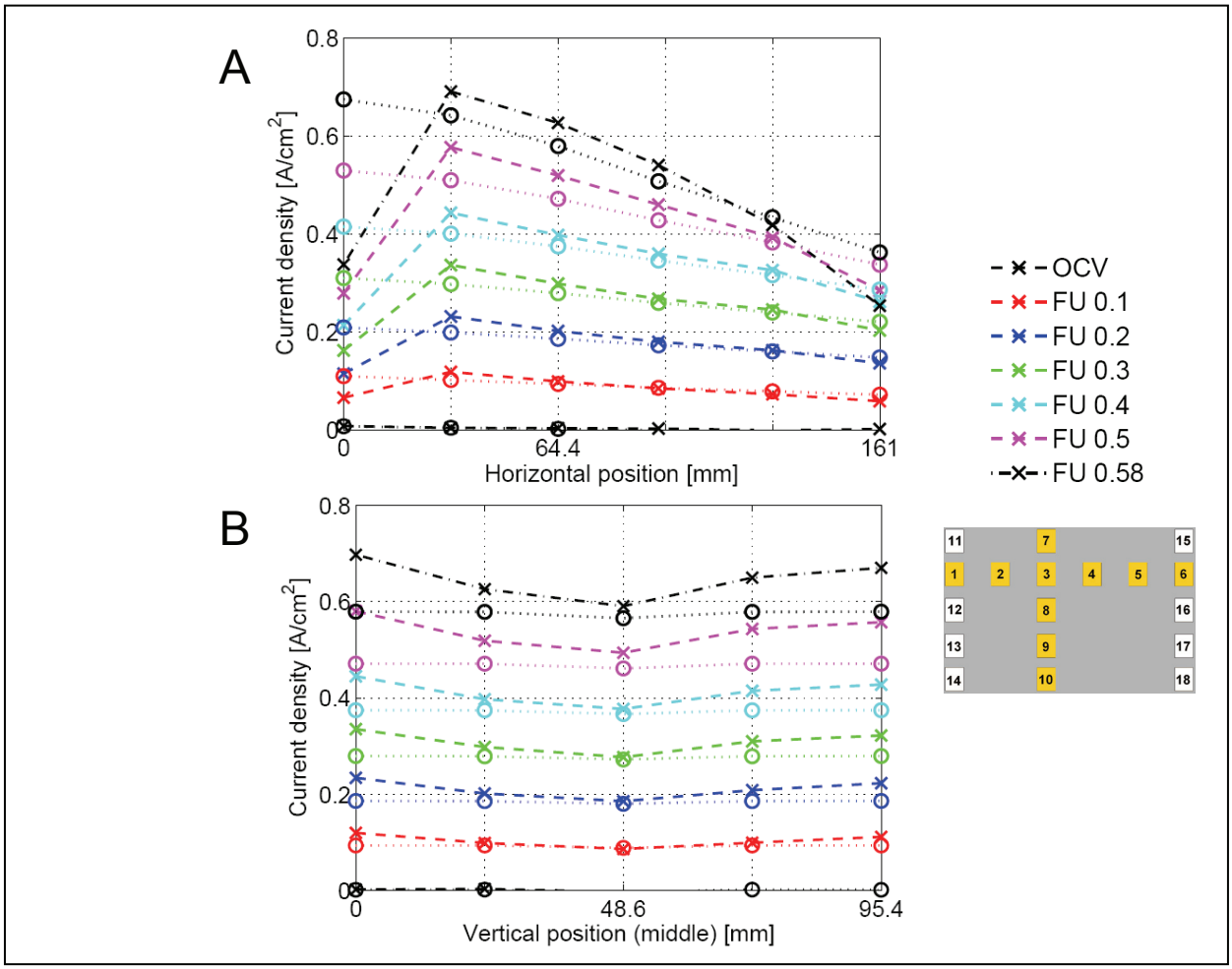

Figure 7: Current density profiles at t=63h as a function of the fuel utilization.
A) along the flow path. B) Across the flow path (second line)
(x) experimental results. (o) simulation outputs

Looking at the transverse direction (Figure 7B) on the second column of segments (3 and 7-10), it can be seen that the current density is up to 16% higher on the sides of the repeat-element than at the center, indicating a mismatch in fuel distribution. The observed current density is higher than the simulation output, as already observed in Figure 7A for the same location along the flow path.

Temperature profiles

For the same operating conditions as the presented current density profiles, the temperature profiles were recorded and compared to simulation outputs (Figure 8). Discrepancies are observed, resulting from simplifications in the modelled geometry (no end-plates, simplified segmented MIC geometry). In addition, the signal for temperature was lost on segment 6, explaining the lack of data.

With an oven temperature of 1073K and an air inlet temperature between 1058 and 1063 K (left), the highest observed temperature is 1085K on segment 4. The small temperature difference between inlet and outlet is explained by the large lambda of 7 and by a large heat transfer between the endplates and the oven. This represents a major difference with a stack configuration.

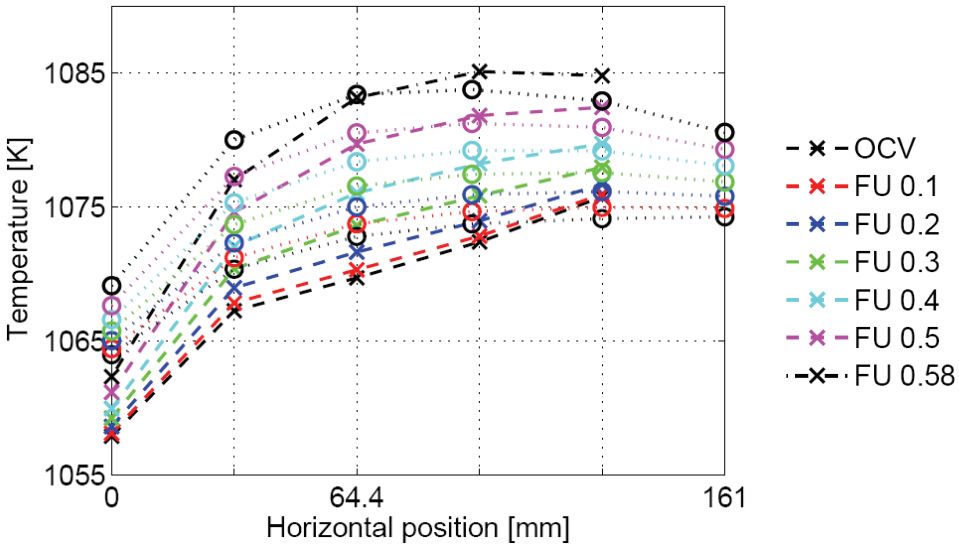

Figure 8: Temperature profiles at different fuel utilizations. (x) experimental results. (o) simulation outputs

Investigations on degradation

Evolution of local performance

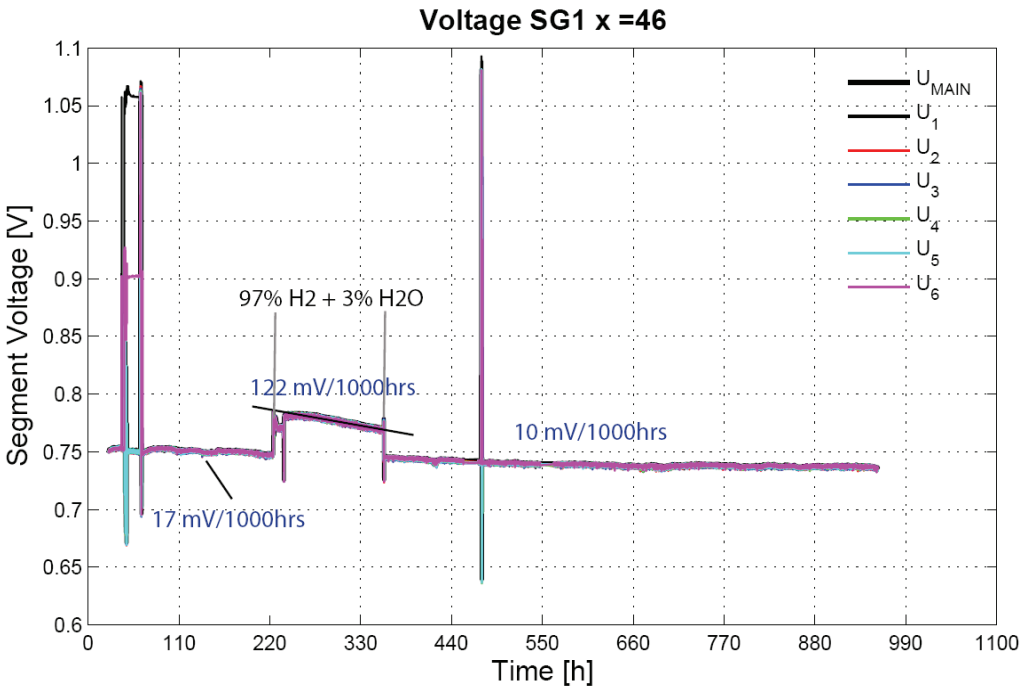

Figure 9: Rates of degradation under various fuel compositions

During the first 220 hours operated at 0,4A/cm2 and 0.753V (average) with a 50% H2 - 50% N2 (+3% H2O) fuel mixture, the degradation was relatively low (-17mV/1000h). When stopping the nitrogen supply to operate under 97% H_2 and while keeping the same current and same fuel utilization, a sudden change in the degradation behavior was observed (Figure 9). The segments with the highest current density (n° 2, 3 and 7 to 10) started to degrade, while the current density increased on other segments, depending on their location along the flow path (Figure 10). Due to the operation at constant current, a balancing effect took place between degrading regions and less affected ones, producing an apparent activation at certain places, but the overall result was a deactivation of -122mV/1000h.

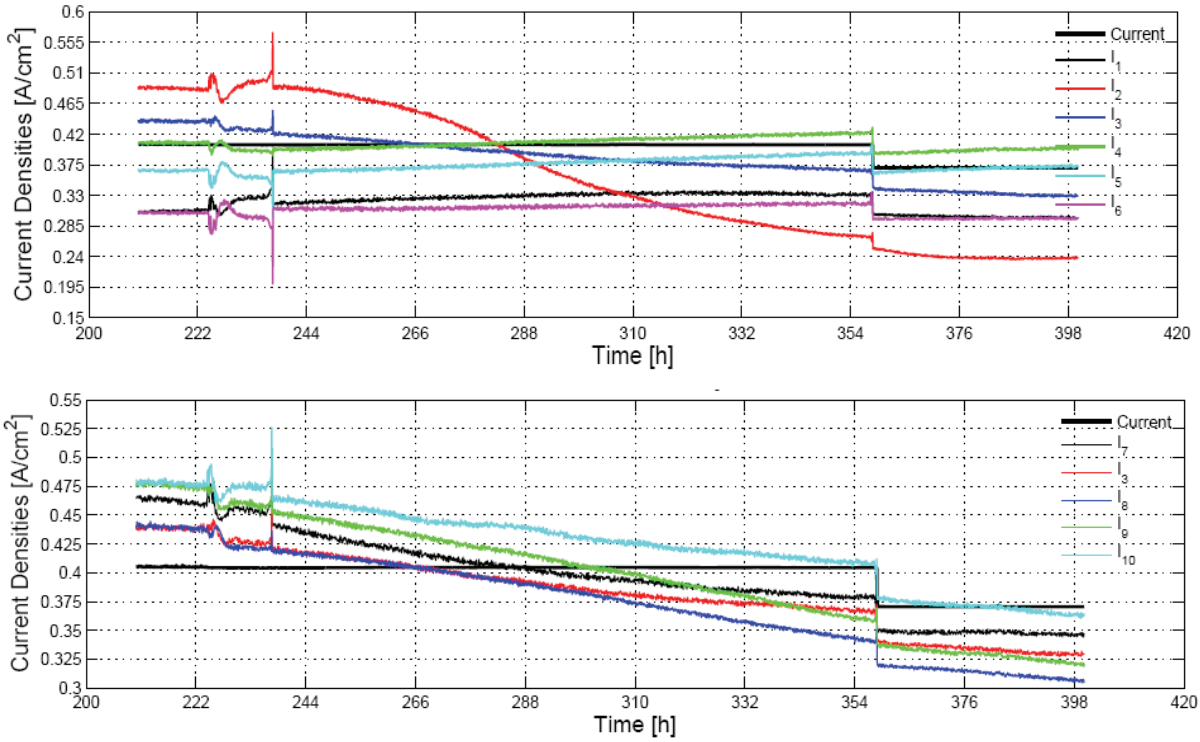

Figure 10 : Evolution of the local current density when changing the fuel mixture from 6SMLPM H2 + 6 SMLPM N2 (+3% H2O) to 6 SMLPM H2 (+3% H2O)

After 130 more hours, the fuel mixture was changed back to 50% H2 - 50% N2 (+3% H2O), for a slightly lower average current density of 0.37A/cm2. No sudden change in degradation behavior occurred this time. In the following 1500 hours, the balancing effect due to degrading regions was well observed, but with a much lower degradation rate of -10mV/1000hours.

Investigation of losses by impedance spectroscopy

After 1600 hours of test, impedance spectroscopy measurements were performed on all segments in order to investigate local degradation processes. To allow comparison between segments, it was necessary to investigate the segment's response under the same operating conditions, i.e. with the same gas composition and same temperature, which is only possible at OCV.
The polarization was therefore stopped. With a slight decrease in OCV of 10mV from inlet to outlet, the gas composition could be considered as nearly equivalent on all segments. The spectroscopy was performed with a bias current of 0.23A/cm^2 in galvanostatic mode, with an AC amplitude of 12mA/cm2. The fuel composition was varied between 50% nitrogen-diluted and pure hydrogen.

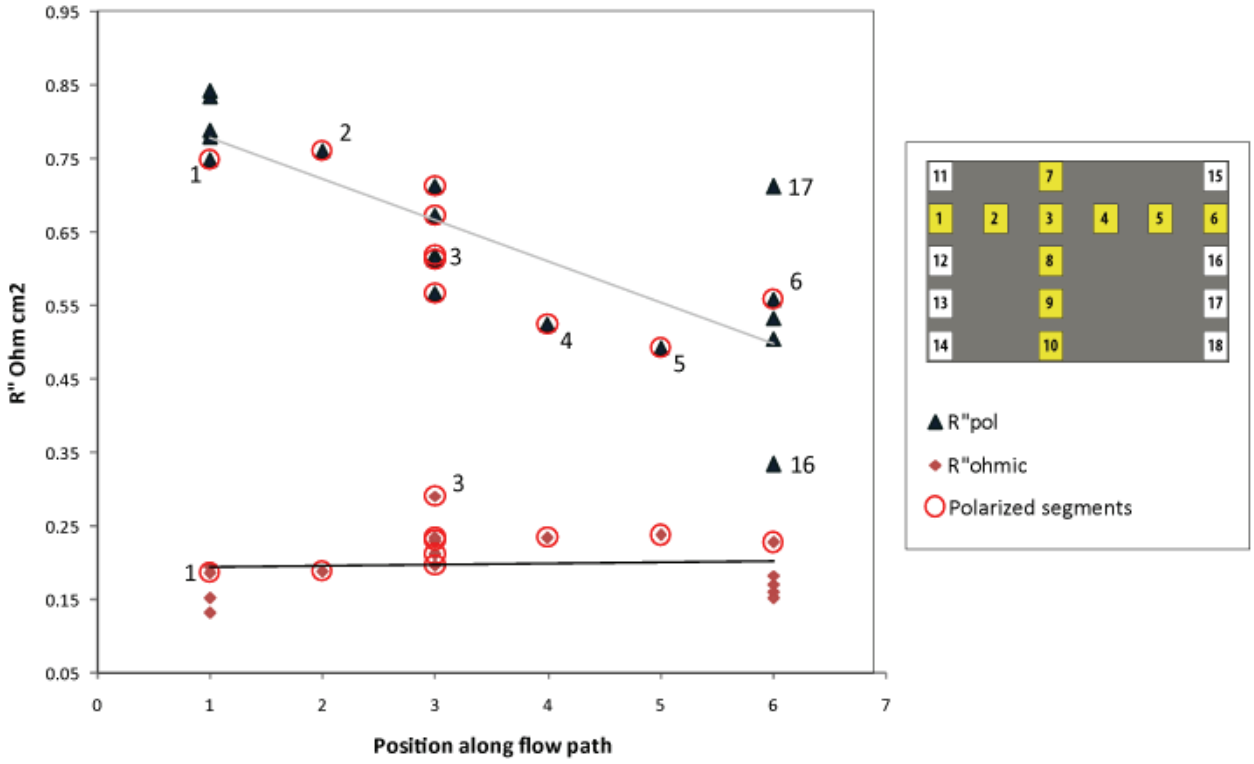

Figure 11: Investigation of ohmic and polarization losses by EIS, as a function of the position along the flowpath.
Conditions: OCV, 6 SMLPM H_2 + 6SMLPM N_2 (+3% H_2), t=1600hrs, 800°C.

Figure 11 shows the results of impedance spectroscopy measurements on the 18 segments with the repeat-element at OCV under diluted fuel. The segments that were polarized during the test are indicated by the red circles. To simplify the lecture, these segments will be called 'polarized' in the following pages, even if the EIS is performed at OCV, while the other will be called 'non-polarized', due to the fact that they were not polarized during the test.

Ohmic resistance

For the polarized segments (1-10), the ohmic resistance is almost constant, with a peak on segment 3 (see Fig. 11, Table 1). The average ohmic resistance for the polarized segments is 224 mOhm cm^2, whereas it is 166 mOhm cm^2 for the unpolarized segments (11-18). An increase in ohmic resistance induced by increasing current density is reported in degradation studies [6], an effect which seems more pronounced at temperatures around 750°C than at higher temperatures. In our case, the effect of polarization on the degradation of the ohmic resistance is visible on the entire element, despite a temperature range between 780°C and 815°C.
These values, which are relatively high, can be partly explained by the use of uncoated F18TNb alloy as interconnector. Finally, segment 1, which showed a poor performance from the beginning of the test, has an ohmic resistance of 186 mOhm cm^2, which is under the average value for the polarized segments, hence excluding a specific contacting problem.

Polarization resistance

The impedance spectra were investigated under pure and diluted fuel, showing differences in the polarization resistance. Results are summarized in Table 1.

		50% H2 + 50% N2 (+3% H2O)			100% H2 (+3% H2O)		
Segment	Position	Rohmic	Rtot	Rpol	Rohmic	Rtot	Rpol
1	1	0.186	0.935	0.749	0.190	0.883	0.693
2	2	0.188	0.949	0.761	0.218	0.879	0.661
3	3	0.291	0.910	0.619	0.296	0.849	0.552
4	4	0.234	0.759	0.525	0.234	0.698	0.464
5	5	0.238	0.730	0.492	0.228	0.665	0.436
6	6	0.227	0.787	0.559	0.227	0.721	0.494
7	3	0.231	0.797	0.566	0.231	0.756	0.525
8	3	0.234	0.906	0.672	0.222	0.848	0.625
9	3	0.197	0.910	0.713	0.197	0.879	0.683
10	3	0.212	0.824	0.612	0.207	0.790	0.583
11	1	0.195	0.975	0.780	0.192	0.957	0.765
12	1	0.132	0.966	0.834	0.122	0.934	0.812
13	1	0.186	0.975	0.788	0.188	0.953	0.765
14	1	0.152	0.995	0.843	0.140	0.964	0.824
15	6	0.183	0.687	0.504	0.173	0.644	0.470
16	6	0.161	0.494	0.333	0.156	0.457	0.301
17	6	0.171	0.882	0.711	0.166	0.836	0.670
18	6	0.152	0.685	0.532	0.148	0.648	0.501

Table 1: ohmic, total and polarization resistances (Ωcm^2) obtained under various fuel compositions

The total resistances are varying from 0.7 to 1.0 Ohm cm2, apart from segment 16 whose apparent better performance remains suspect (possible electrical contact to the main segment). These large ASR are partly due to the degradation that occurred during the test, but also due to the experimentation point at OCV with low steam content (steep drop of Nernst potential).
Figure 11 shows that the polarization resistance of the polarized segments (1-10) decreases by 35% from inlet to outlet. It indicates a large difference in the degradation behavior, which is studied in more details thereafter.
It has to be noted that the current density profiles, as shown in Figure 7, changed to a large extent during the test, with a large decrease in current density, near the inlet (segments 2 and 3). With an already large polarization resistance on segment 1 at the inlet after only 63 hours of operation, it can indicate for example a pollution of the cathode from

upstream components. However, for the segments located at the inlet (1, 11, 12, 13, 14), the polarization resistances are in a relatively close range. The lowest value on the polarized segment, which can indicate an activation process.
For the segments at the outlet (15, 6, 16, 17 and 18), large variations are observed. While the non-polarized segments 15 and 18 (in the corners) have polarization resistances close to the one of the polarized segment 6, the segment n°17 shows a large polarization resistance, and segment 16 a value which is well below the average.

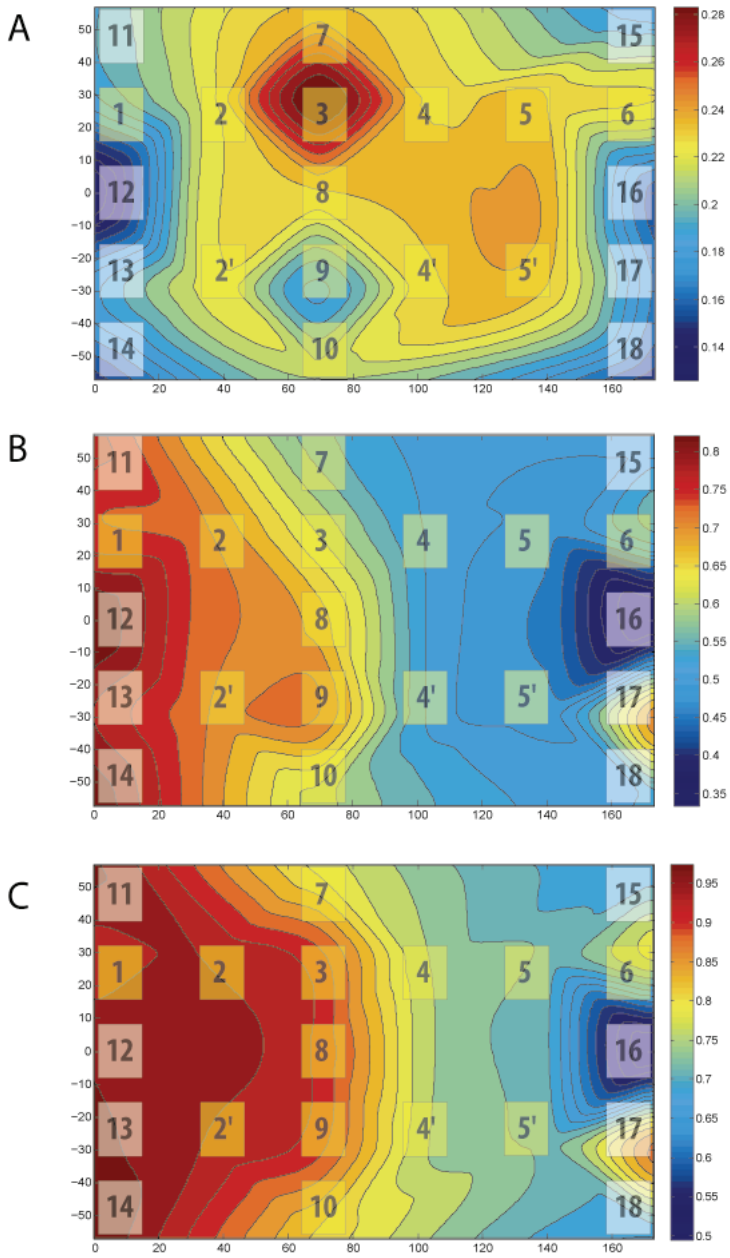

Figure 12: Local results from EIS measurements at OCV. (A) Ohmic resistance (Ω cm^2), (B) Polarisation resistance (Ω cm^2), (C) Total resistance (Ω cm^2). Conditions: OCV, 6 SMLPM H_2 + 6SMLPM N_2 (+3% H_2), t=1600hrs.

As a summary of EIS results, maps of the various impedance contributions are plotted over the active area. Figure 12 shows the resulting figures, hence indicating the areas affected by degradation. The segments 2, 4 and 5 are mirrored over the horizontal symmetry axis. It can be clearly seen that the polarization losses (B) and therefore also the total ASR (C) strongly decrease from inlet to outlet, giving precious information for the future post-experiment analysis.

Contributions to the polarization resistance

In order to separate the various contributions to degradation processes, an analysis of the recorded spectra was performed, following the methodology described by Hagen et al. in [6]. Typical variations in the Nyquist plots are observed, completed by an analysis of the imaginary part of the impedance over the frequency domain. Variations in fuel compositions are used to attribute the observed response either to anode or cathode side.

Figure 13 shows the Nyquist plot of the impedance spectra recorded at OCV on the 18 segments after 1600 hours of operation. Polarized segments are identified by red markers, non-polarized by blue ones. The segments that were polarized during the test clearly show larger ohmic resistances.

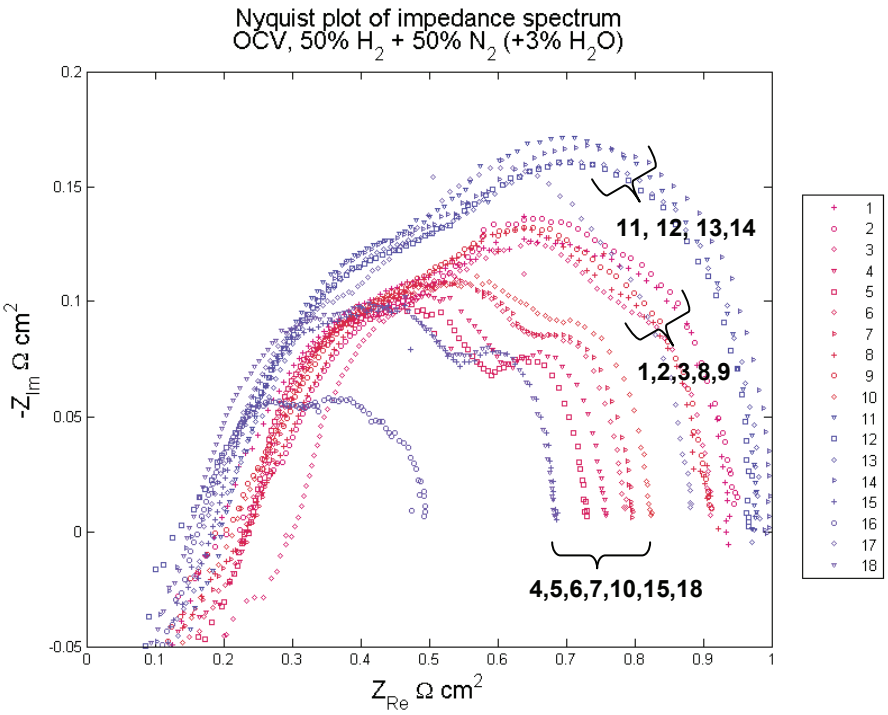

Figure 13 : Nyquist plot of the impendance spectra recorded on all segments. Polarized segments are indicated in red, non-polarized ones in blue. Conditions: OCV, 6 SMLPM H_2 + 6SMLPM N_2 (+3% H_2), t=1600hrs, 800°C.

Three different groups with similar impedance spectra are visible.
The ***first group***, with the lowest total impedances, consists of segments (4-7,10,15,18), all situated in the second half of the repeat-element towards the outlet (see map on Figure 12B) and along the sides. Not all of these segments were polarized. For this group, the Nyquist plot shows a distinct small arc in the low frequency region.
The ***second group***, with intermediate total impedance, consists of the segments 1-3, 8 and 9, all polarized and located in the first half of the repeat-element, towards the inlet. The low frequency arc is larger than the one of the first group, while the behaviour remains similar at higher frequencies.
The ***third group***, showing the largest total impedance, consists of the segments 11 to 14, all being not-polarized, and all located at the inlet.
Segment 16 is clearly below the other segments, while segment 17 shows intermediate values.

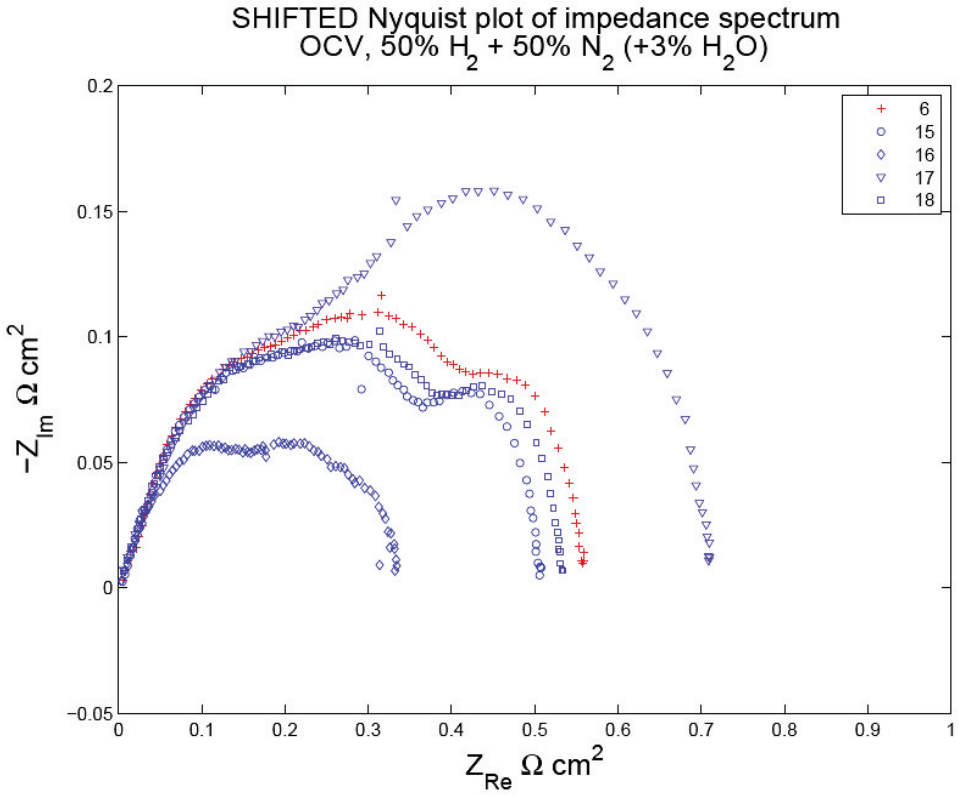

Figure 14: Nyquist plot of the corrected EIS spectra of the outlet segments (removal of serial resistance and inductance). Conditions: OCV, 6 SMLPM H_2 + 6SMLPM N_2 (+3% H_2), t=1600hrs.

An interesting information is given by the segments located at the outlet. By subtracting the evaluated serial resistance and inductance of the equivalent circuit, the Nyquist plots of the polarization resistance can be compared, as shown in Figure 14. It shows that the polarization losses of the polarized segment 6 are only slightly higher than the ones of the non-polarized segments 15 and 18 located in the corners, and this with a very similar impedance spectrum. In this case again, it indicates that the observed degradation depends a lot on the position in the repeat-element, and less on the polarization.
Apart from segment 16, which is suspected to have had an electrical contact to the main segment, segment 17 shows an interesting large semi-circle at intermediate frequencies. Post-experiment analyses will therefore be performed to compare this segments to the other ones at the same location, in order to investigate which electrode might have been affected.

Investigations over the frequency domain

To illustrate the various degradation processes, an analysis of the Bode plot of the imaginary part of the impedance spectra is performed. As shown by Barfod and Hagen [6, 7]., It allows to separate the contributions to the polarization resistance. Peaks of the imaginary part ($-Z_{im}$), and the associated frequencies, indicate the presence of characteristic semi-circles in the Nyquist representation, of parallel resistance/constant phase elements in an equivalent circuit, and of a specific interface or process in an operating fuel cell.
The response in $-Z_{im}$ of the 18 segments is summarized in Figure 15. As the temperature and the gas composition is kept constant over the segments, it clearly illustrates various degrees of degradation over various frequency ranges.

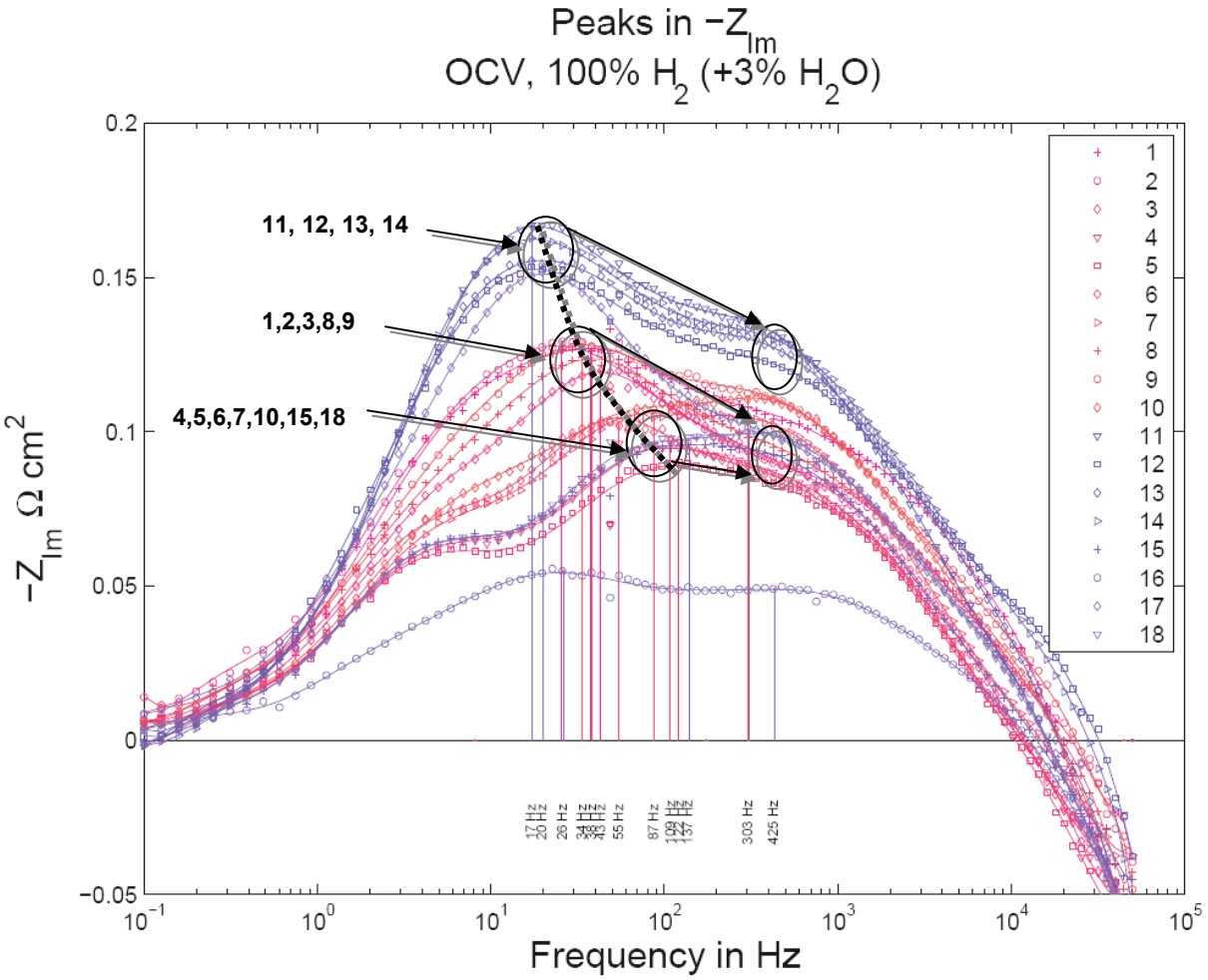

Figure 15: Study of the frequency response of the segments under constant conditions after degradation. Bode plot of the imaginary part of impedance of the 18 polarized (red) and non-polarized (blue) segments. Frequencies associated to local maxima of $-Z_{im}$. Conditions: OCV, 6 SMLPM H_2 + 6SMLPM N_2 (+3% H_2), t=1600hrs.

Large differences are observed in a frequency range from 1Hz to 5kHz, in particular in the range 5 to 200Hz, and to a lower extent up to 1kHz. A number of peaks are easily visible, differing from one segment to another. In order to identify the characteristic frequencies, the peaks present in the whole set of data were identified numerically, as local maxima.

The three characteristic groups of segments identified previously by analyzing the Nyquist plots are again visible (see Figure 15), with common peaks in the mid-frequency range (17-110Hz). The peaks found in this frequency range can be located on a continuous line.

It is therefore possible that this group of frequencies corresponds in fact to the same interface or process, but at different levels of degradation. In fact, a more degraded interface or process should produce wider semicircles in the Nyquist plot, higher peaks of the imaginary part and also a shift towards lower frequencies.
The first group, with the best performance, shows a distinct peak at 4Hz. Large variations are observed among the other groups at this frequency, with a possible overlapping with the peaks located in the mid-frequency range.
Another peak is present around 300-400Hz, where groups 1 and 2 present similar values. The 3rd group, located at the fuel cell inlet, shows a higher value in this range.

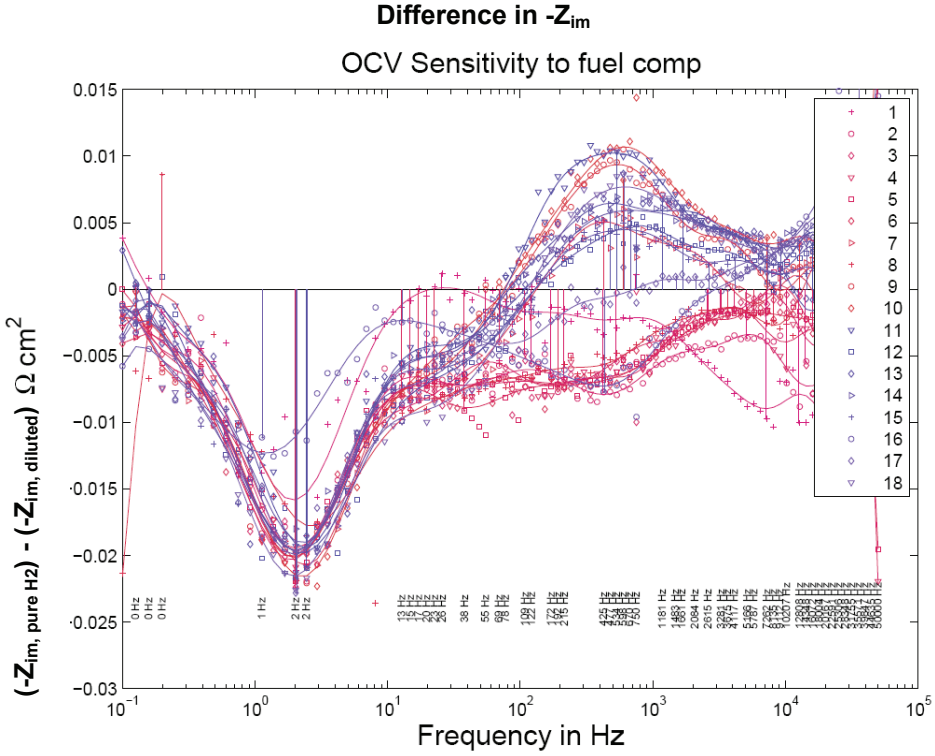

Figure 16 : Bode plot of sensitivity of the impedance to the fuel composition (($-Z_{pure\ H2}$)- ($-Z_{dilute\ fuel}$))

To attribute the peaks to the different contributions to the polarization resistance, variations of the fuel composition were performed. Figure 16 shows the difference in $-Z_{im}$ when changing the fuel composition from pure to dilute fuel. It reveals the presence of variations in distinct frequency domains.

- From this analysis, it can be seen that the *low frequency peaks* (4Hz) are sensitive to the fuel composition, hence probably originating from gas conversion processes.
- In the *mid-frequency range*, the sensitivity of the peaks to the fuel composition is low. Still, more analyses are needed to attribute it to the cathode side.
- Finally, another important variation is observed at *high frequencies* around the 300-400Hz peaks, whereas with an increase in $-Z_{im}$ for certain segments, and a decrease for others.

Coming back to local degradation in the repeat-unit, a local analysis can be performed by plotting maps of the impedance as function of the frequency domain. As an example, the peaks of the imaginary part of impedance ($-Z_{im}$) can be plotted for a specific frequency range attributed to one specific interface or degradation phenomenon.
An example is given in Figure 17 for the peaks of the imaginary part of impedance ($-Z_{im}$) detected in the mid-frequency range. From the present analysis, it can be seen that the peaks present in the mid-frequency range show the highest maxima and the largest

variations in $-Z_{im}$, and represent therefore a major contribution to the overall degradation in this test. Therefore, it has to be confirmed whether these peaks belong to the same phenomenon or interface.
The resulting map allows to perform dedicated local post-experiment analyses in order to confirm the hypothesis, and to make a link to impedance data.
As shown in Figure 17, the map obtained for this frequency range shows a clear decrease in $-Z_{im}$ from inlet to outlet, in a similar way as the total impedance reported above (Figure 12). This indicates a probable common phenomenon.

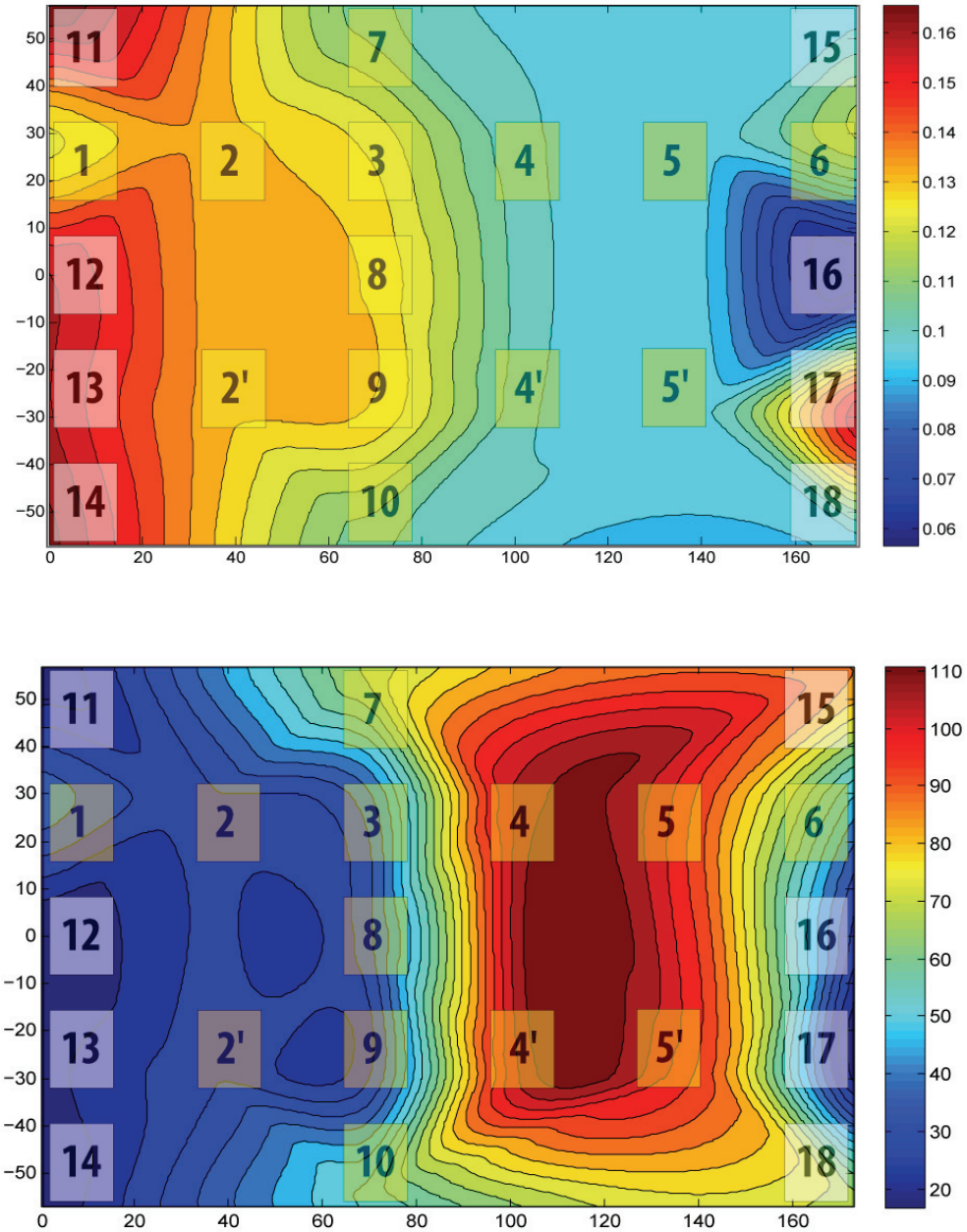

Figure 17 : Maps of peak values of $-Z_{im}$ (TOP) and corresponding peak frequency (BOTTOM) in the frequency range 15Hz to 150Hz. Conditions: OCV, 6 SMLPM H_2 + 6SMLPM N_2 (+3% H_2), t=1600hrs, bias current 400mA.

Conclusion and outlook

The segmented experiment presented here has allowed to study at various levels the local performance and local degradation behavior of a repeat-element in operation. It has allowed to detect performance limitations due to some mismatch in fuel distribution, an information that would have been difficult to obtain in a less instrumented experiment.
The rich data collected by the local current density measurements has put in evidence localized degradation phases, accompanied by a redistribution of the electrochemical reaction over the whole active area, an information that is not available in another test configurations.
The impedance spectroscopy measurements have allowed to study more in details the various contributions to the electrochemical losses, showing different trends over the active area. The large number of segments was in this sense of great interest, as it allowed to detect several different contributions to the degradation, as well as different degradation levels for specific phenomena. The established degradation maps will allow to focus the following post-experiment analysis on specific regions of interest. In addition, the presence of non-polarized segments has allowed to identify some contributions of the polarization on the degradation.
Nevertheless, more work has to be done to clarify the causes of degradation and in particular to make a link to the impedance data. Post-test analyses will be performed based on these preliminary results.
With this new diagnostic tool, next experiments should allow to investigate more in depth the degradation processes of SOFC's, and hopefully help to increase their lifetime.

Acknowledgements

The authors would like to thank all persons who actively participated to the creation of this new diagnostic test station, both at EPFL and at HTceramix SA - SOFCpower. Sincere thanks also to the FP6 European Project 'FlameSOFC' (FP6-SES6-19875) and to the Swiss National Science Foundation (SNF n°200020-109-643) for funding.

References

1. Ravussin, F., et al., *Local current measurement in a solid oxide fuel cell repeat element.* Journal of the European Ceramic Society, 2007. **27**(2-3): p. 1035-1040.
2. Metzger, P., et al., *SOFC characteristics along the flow path.* Solid State Ionics, 2006. **177**(19-25): p. 2045-2051.
3. Larrain, D., et al., *Generalized model of planar SOFC repeat element for design optimization.* Journal of Power Sources, 2004. **131**(1-2): p. 304-312.
4. Wuillemin, Z., et al., *Modeling and Study of the Influence of Sealing on a Solid Oxide Fuel Cell.* Journal of Fuel Cell Science and Technology, 2008. **5**(1): p. 011016-9.
5. Nakajo, A., et al. *Determination of an electrochemical model from experiments on a segmented solid oxide fuel cell*. in *3rd fuel cell research symposium on modelling and experimental validation*. 2006. Dübendorf, Switzerland: EMPA.
6. Hagen, A., et al., *Degradation of Anode Supported SOFCs as a Function of Temperature and Current Load.* Journal of The Electrochemical Society, 2006. **153**(6): p. A1165-A1171.
7. Barfod, R., et al., *Detailed Characterization of Anode-Supported SOFCs by Impedance Spectroscopy.* Journal of The Electrochemical Society, 2007. **154**(4): p. B371-B378.